High-Performance Filaments from Compatibilized Polypropylene/Clay Nanocomposites

M. Joshi, V. Viswanathan

Department of Textile Technology, Indian Institute of Technology, Hauz Khas, New Delhi, 110 016, India

Received 30 June 2005; accepted 12 January 2006
DOI 10.1002/app.24179
Published online in Wiley InterScience (www.interscience.wiley.com).

ABSTRACT: Polypropylene (PP)/nanoclay composite filaments were produced by melt spinning and characterized to study the effect of the compatibilizer and the role of the nanoclay in improving the physical properties. The compatibilizer was maleic anhydride grafted PP. Clay loadings up to 1 wt % with up to 3 wt % compatibilizer were explored. There was a significant improvement in the tensile, thermal, and dynamic mechanical properties and creep resistance of PP/nanoclay composite filaments over neat PP filaments at very low clay loadings of 0.25–0.5 wt % and a compatibilizer/clay ratio of 2:1. The properties were correlated to the morphology of the nanocomposite filaments, which was investigated with differential scanning calorimetry, X-ray diffraction, and transmission electron microscopy. © 2006 Wiley Periodicals, Inc. J Appl Polym Sci 102: 2164–2174, 2006

Key words: compatibilization; drawing; fibers; nanocomposites; poly(propylene) (PP)

INTRODUCTION

The growth of polypropylene (PP) as a technical textile material has been quite noteworthy, primarily because of its low cost, inert nature, low density, hydrophobic nature, excellent resistance to chemicals and biological organisms, and wide range of physical properties. However, some of its shortcomings are a low-use temperature, difficulty with dyeing, poor UV resistance, and a tendency to creep at and above room temperature.[1] The recent tremendous success of polymer/clay hybrid nanocomposites offers attractive potential for the continuous expansion of the application versatility of PP for industrial textile use.

There has been intense interest in this field[2,3] of polymer nanocomposites ever since the Toyota research group demonstrated the enhanced properties of nylon 6/nanoclay composites. The most promising ones seem to be those using montmorillonite (a 2 : 1 phyllosilicate) as the reinforcing agent. Most of these polymer/nanoclay composites have shown excellent properties, such as high tensile strength and modulus, high heat distortion temperatures, and low gas permeability.[4–9] Melt intercalation is becoming an attractive route for synthesizing polymer/clay nanocomposites because of the several advantages that it has over other methods such as solution intercalation and intercalation polymerization.[10] It is environmentally friendly because of the absence of solvents and is also compatible with current industrial mixing and processing techniques.[2,11] Besides, melt mixing[12–14] with a twin-screw extruder and injection molding are economical and can break up the clay platelets more easily than other specialized techniques.

PP/clay nanocomposites[12,13,15,16] have attracted great attention from researchers because they exhibit properties such as improved tensile strength and modulus, enhanced storage modulus, decreases in tan δ, and dramatic increases in the crystallization rate. The silicate clay layers have polar hydroxyl groups and are incompatible with olefins, which are nonpolar and unreactive. Hence, polar oligomers such as functionalized PP are used for enhancing the compatibility between the clay and the polymer matrix.[16,17] Most of these studies on PP/clay nanocomposites have been performed on polymers in film or mold form, whereas studies on the filament form have not been widely reported. There have been two recent reports on nanocomposite fibers based on a PP/clay system.[18,19] Borsig et al.[18] reported the melt spinning of nanocomposites prepared from syndiotactic polypropylene (SPP) and organolayered silicate (M-ODA) with maleic anhydride grafted isotactic polypropylene (iPP-*g*-MA) as a compatibilizer. Transmission electron microscopy (TEM) has been applied to monitor the development of the morphology during spinning and correlated to improvements in the properties. Another study[19] reported an interesting finding on increased crystallinity, decreased orientation, and increased moisture absorption for PP/organically modified montmoril-

Correspondence to: M. Joshi (mangala@textile.iitd.ernet.in).
Contract grant sponsor: Indian Ministry of Human Resource Development (through a research project).

TABLE I
Master Batch Composition

Sample	PP (%)	Nanoclay (%)[a]	Compatibilizer (%)[b]
PP	100	0	0
Master batch 1	85	5	10
Master batch 2	95	5	0
Master batch 3	0	5	95

[a] Cloisite 15A.
[b] Fusabond MD511D.

lonite (OMMT) hybrid fibers but observed many flaws on the fiber surface. That study used a higher OMMT concentration of 5 wt %, maleic anhydride grafted polypropylene (PP-*g*-MA; ~ 2 wt %) as the compatibilizer, and polystyrene (~ 1 wt %) along with neat PP (~ 100 wt %).

This study investigates the preparation of compatibilized PP/nanoclay composite filaments with a focus on the effect of clay on the melt spinning and drawing of nanocomposites into oriented filaments and their characterization for mechanical, dynamic mechanical, and thermal properties and shrinkage behavior. The property correlation to the developed morphology has been investigated with differential scanning calorimetry (DSC), X-ray diffraction, and TEM. This is a continuation of our earlier work on uncompatibilized PP/nanoclay filaments.[20] The unique part of this study is that at very low clay loadings (< 1 wt %), remarkable improvements in the properties have been obtained in comparison with the higher loadings (1.5–5 wt %) used in previous studies.[18,19]

EXPERIMENTAL

Material

Isotactic PP [Koylene ADL (AM120N); melt flow index (MFI; g/10 min) = 12] was procured from IPCL (Vadodara, India). Cloisite 15A (OMMT) was procured from Southern Clay Products, Inc. (USA). It had an ion-exchange capacity of 125 mequiv/100 g and a specific density of 1.66 g/cc. The typical clay particle size (for 90% of the particles) was less than 13 μm. Fusabond MD511D (PP functionalized with maleic anhydride; medium grafting level) was supplied by DuPont Canada, Inc. It had a medium grafting level with an MFI (g/10 min) of 24 and a melting point of approximately 162°C.

Preparation of the master batches

Master batches containing 5 wt % clay and a PP/PP-*g*-MA mixture were prepared on an SDL-Atlas F255A-D laboratory mixing extruder from SDL Atlas (England). This laboratory mixing extruder had an automatic rotor and temperature control with a variable speed of 5–260 rpm, a 1/8-in. (3-mm) orifice, and a water-cooled hopper. The compositions of the master batches are given in Table I. The rotor and die zone temperatures were kept at 200 and 260°C, respectively, and the rotor speed was set at 152 rpm.

Preparation of the nanocomposite filaments

Spinning

The nanocomposite filaments were melt-spun on a laboratory single-screw extruder (length/diameter = 25) from Betol Machinery Ltd., UK, under the optimized spinning conditions, that is, a screw speed ranging from 5 to 10 rpm and a haul-off speed varying from 6 to 18 m/min with a die orifice diameter of 1 mm. The temperatures for the four zones were kept at 210, 230, 240, and 260°C. The sample code PPc*X*g*Y* stands for a sample containing PP, (*X*/10) wt % clay and (*Y*/10) wt % compatibilizer. Samples with various clay contents (0.25, 0.5, and 1.0 wt %) and clay/compatibilizer ratios of 1 : 1, 1 : 2, and 1 : 3 were prepared. The sample codes and compositions are given in Table II.

Drawing

The extruded filaments were drawn on a laboratory drawing machine with a three-stage drawing process at 80, 110, and 150°C. All the filaments were fully drawn, that is, to an extent beyond which the filaments turned white with further drawing.

Characterization

Thermogravimetric analysis (TGA)

The TGA studies were carried out on a PerkinElmer TGA7 instrument from Perkin Elmer Life and Analytical Sciences, Inc. (USA). The heating rate was 20°C/

TABLE II
Sample Codes and Compositions

	Sample composition	
Sample code	Clay (wt %)	Compatibilizer (wt %)
PP	0	0
PPc025g00	0.25	0
PPc05g00	0.5	0
PPc10g00	1.0	0
PPc00g10	0	1.0
PPc00g20	0	2.0
PPc025g025	0.25	0.25
PPc025g05	0.25	0.50
PPc025g075	0.25	0.75
PPc05g05	0.50	0.50
PPc05g10	0.50	1.00
PPc05g15	0.50	1.50
PPc10g10	1.00	1.00
PPc10g20	1.00	2.00
PPc10g30	1.00	3.00

min for all the samples, and the temperature ranges were 30–900°C (clay), 50–500°C (compatibilizer), and 50–600°C (nanocomposite filament).

DSC

DSC studies of the compatibilizer and PP/clay composites filament samples were carried out on a Perkin-Elmer DSC-7 instrument from 50 to 200°C at 10°C/min under a nitrogen atmosphere. The melting temperature (T_m) and crystallization temperature of the compatibilizer determined by DSC were 166 and 123.9°C, respectively.

The crystallinity of the samples was calculated with the following formula:

$$\chi_c = \Delta H/\Delta H^0_{pp} \quad (1)$$

where ΔH is the enthalpy of fusion of the sample (J/g) and ΔH^0_{pp} is the enthalpy of fusion of completely crystalline PP ($\sim$ 209 J/g).

X-ray diffraction studies

Wide-angle X-ray (WAXD) studies were performed on a Philips PW 1730/10 diffractometer with Ni-filtered Cu Kα radiation (1.5418 Å) from Philips PANalytical B.V (The Netherlands). Scanning was carried out in the 2θ range of 10–35° at 2°/min. Small-angle X-ray studies from 2 to 15° at 10°/min were carried out on a Bruker (D8 Advanced) diffractometer from Bruker AXS Inc. (USA). X-ray crystallinity was calculated from a plot of the intensity versus 2θ. The formula used for the calculation of the degree of crystallinity (X_c) was

$$X_c = [I(t) - I(a)]S^2/I(t)S^2 \quad (2)$$

where S is equal to $n\,\lambda/2 \sin\theta$ (per Bragg's law) and $I(t)$ and $I(a)$ are the total and amorphous intensities, respectively.

WAXD was used to determine the crystallinity and crystalline orientation of the filaments. Herman's orientation function (f_c) for the filaments is defined as follows:

$$f_c = (3\cos^2\theta_{hkl,z} - 1)/2 \quad (3)$$

where $\theta_{hkl,z}$ is the angle between the reference direction (filament axis) and the X-ray crystallographic axis. Assuming rotational symmetry about the filament axis, we find

$$\cos^2\theta_{hkl,z} = \sum I(\theta)\cos^2\theta \sin\theta d\theta / \sum I(\theta)\sin\theta d\theta \quad (4)$$

where $I(\theta)$ is the intensity of diffraction from the (hkl) planes, which are normal to the X-ray crystallography direction. The summations in the equation are evaluated numerically from the intensity distribution of the (110) and (040) reflections.

For monoclinic PP

$$f_c = (3\cos^2\theta_{c,z} - 1)/2 \quad (5)$$

where $\cos^2\theta_{c,z}$ is equal to $1 - 1.099\cos^2\theta_{110,z} - 0.901\cos^2\theta_{040,z}$ and $\cos^2\theta_{110,z}$ and $\cos^2\theta_{040,z}$ are obtained from the azimuthal intensity distribution measurements of (110)and (040) from eq. (4).

TEM

Microscopy investigations were performed on a Philips CM-12 transmission electron microscope operating at 80 kV. The thin sections ($\sim$ 100 nm) of the filaments were obtained with a cryoultramicrotome and placed on grids, which were mounted in a sample holder, and the brightness of the electron beam was minimized to prevent damage to the samples.

Sonic modulus measurement

The sonic modulus is a measure of the overall molecular orientation and was measured on a PPM-5R tester made by HMM Morgan Co. (USA). The sonic modulus was calculated with the following formula:

$$E = 11.3C^2 \quad (6)$$

where E is the modulus in grams per denier (gpd); 1 gpd $\sim \rho \times 8.83 \times 10^7$ Pa, where ρ is the density and C is the sonic velocity (km/s). Denier is a unit for the linear density of fibers equivalent to the weight in grams of 9000 m of the fiber.

Thermomechanical analysis (TMA)

TMA of the filament samples was carried out on a PerkinElmer TMA-7 instrument. The samples were heated from 50 to 150°C at 10°C/min under a constant load of 0.05 gpd, and the shrinkage in the samples was determined.

Boiling water shrinkage

The filaments were exposed to boiling water at 100°C for 30 min under free conditions without tension. The shrinkage in length was noted and gave an indication of the thermal stability of the samples to hot and wet environments.

Tensile testing

Tensile testing of the filaments was carried out on a Statimat ME tester from Textechno, GmbH & Co. (Germany). The gauge length was 100 mm, and the strain rate was kept constant at 35 mm/min. Ten specimens were tested for each sample, and the average value was reported. The coefficient of variation for all samples was within 5%.

Dynamic mechanical analysis

A PerkinElmer DMA 7 was used for the dynamic mechanical testing of the prepared filaments. The tests were carried out at 1 Hz and at a heating rate of 10°C/min for all the samples in the tensile mode.

Creep testing

Pure PP and nanocomposite filaments were subjected to creep testing to determine their long-term mechanical stability. The filaments were subjected to 20% of their breaking load, and the readings were taken at frequent intervals up to 45 h with a cathetometer to determine the creep setting.

RESULTS AND DISCUSSION

Spinning and drawing

Melt spinning is the most popular technological method of producing filaments. The orientation of macromolecules along the flow direction occurs partly because of extensional shear flow in the spinneret channels and develops gradually along the spinning path because of elongation in the fluid filament. The drawing or orientation stretching process is vital for textile applications for increasing the strength of polymeric fiber and films. During drawing, the fiber/filament is further strengthened by the alignment of molecular chains along the fiber axis. Drawing also induces changes in the level of crystallinity and sometimes in crystalline forms. An increase in the draw ratio results in an improvement of the orientational order and hence the properties. However, the limiting value of this draw ratio is dependent on the prehistory of the polymer and drawing conditions. The termination of drawing may be due to random defects and changes in the supramolecular structure, which finally lead to local overstresses due to the structural heterogeneity along the orientation axis.

The neat PP and nanocomposite filaments were spun by melt extrusion and drawn to produce fully drawn filaments. The drawability values attained with the various compositions are given in Figure 1. The addition of the nanoclay to the PP matrix hindered the drawing process. Although a maximum draw ratio of 13 was achieved for neat PP, it was reduced to 9 for uncompatibilized PP/clay filaments with a 0.5 wt % clay loading. In the absence of the compatibilizer, the presence of clay tactoids restricted the mobility of the chains by acting as points of local overstresses and hindered the process of chain alignment, thereby leading to a decrease in the drawability. However, upon the addition of the compatibilizer, the drawability improved and approached the draw ratio attained with neat PP ($\sim$ 13) and even exceeded it in some cases. This could be attributed to the better dispersibility and intercalation/exfoliation of the clay platelets in the PP matrix in the presence of the compatibilizer, as was also evident from a TEM investigation (Fig. 2). The TEM photographs reveal that silicate layers were uniformly dispersed in the polymer matrix and that the layers were exfoliated or intercalated in the presence of the compatibilizer, which provided excellent spinnability to the PP/clay compatibilized system at a low clay concentration of ($<$ 1 wt %). In this study, nanocomposites with clay concentrations of more than 1% could not be melt-spun because of excessive breakage during spinning.

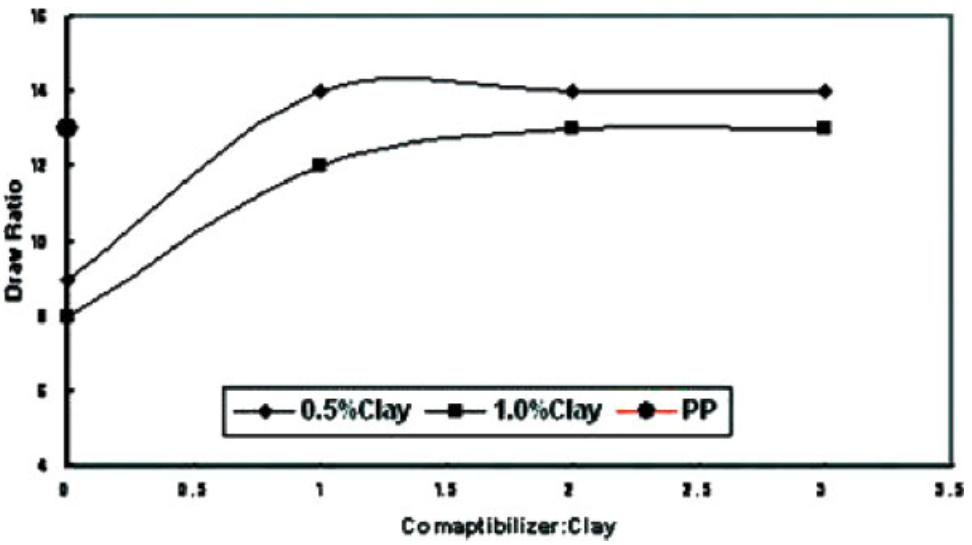

Figure 1 Drawability of PP and PP/clay nanocomposite filaments with various compatibilizer/clay loadings. [Color figure can be viewed in the online issue, which is available at www.interscience.wiley.com.]

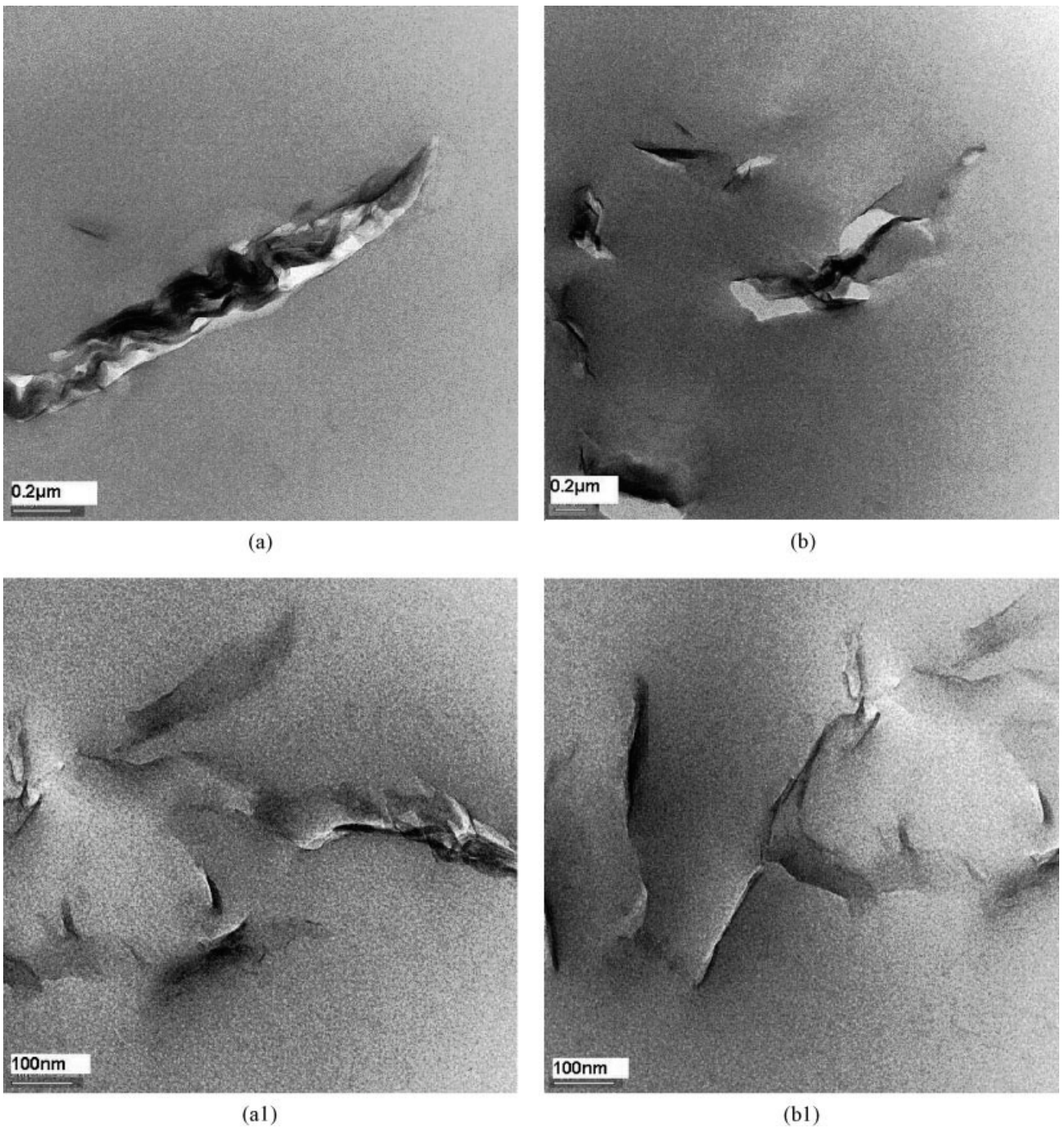

Figure 2 TEM micrographs of PP/clay nanocomposite fibers: (a & b) uncompatibilized with 0.5 wt % clay and (a1 & b1) compatibilized with 0.5 wt % clay and 1 wt % compatibilizer.

However, Borsig et al.[18] in their study on SPP/OMMT hybrid fibers reported that although drawability ($\lambda \sim 2$–3) was facilitated in the presence of a compatibilizer (low-molecular-weight iPP-*g*-MA), the tensile strength for all SPP/OMMT fibers was lower than that of uncompatibilized OMMT-filled SPP fibers. This was because of the negative influence of the low molecular weight of the compatibilizer affecting both the crystallinity and polymer chain orientation.

Crystallinity and orientation

X-ray diffraction studies

The clay showed a characteristic peak between 2.6 and 3° corresponding to a *d*-spacing of 3.48 nm, whereas in the case of the nanocomposites, there was no evidence of this peak [Fig. 3(a)]. In fact, for the nanocomposites, the first peak was seen around 14°, which is characteristic of PP crystals. The absence of the peak may have

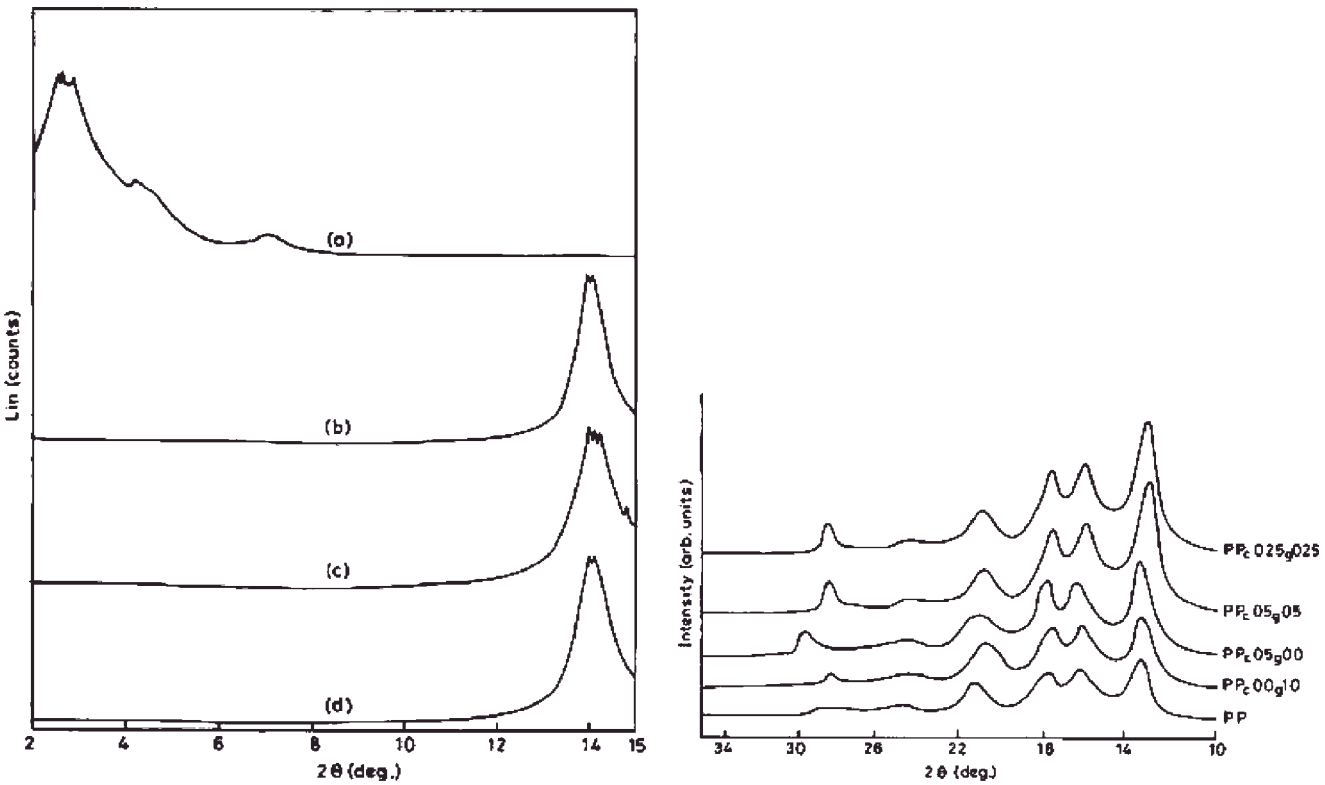

Figure 3 (a) X-ray diffractograms ($2\theta \sim 1.5$–10°) for (a) Cloisite 15A, (b) PPc025g025, (c) PPc05g05, and (d) PPc10g10 and (b) X-ray diffractograms ($2\theta \sim 10$–35°) for PP and PP/clay nanocomposite filaments.

indicated either a disordered intercalated or exfoliated clay dispersion in the nanocomposites, as also suggested by other researchers of PP/nanoclay composites.[21] The wide-angle X-ray diffractograms in the 2θ range of 10–35° are given in Figure 3(b). The addition of the nanoclay to the PP matrix produced no changes in the characteristic peak positions of PP, and this indicated that the addition of the nanoclay to the PP matrix does not affect the basic crystal structure of PP in the drawn filaments.

The X-ray crystallinity and crystalline orientation values for the samples are given in Table III. Upon the addition of the nanoclay to the PP matrix, there was initially a drop in the crystallinity values, but the values went up in the samples with the compatibilizer. As the clay loadings were increased, higher compatibilizer/clay ratios were required to achieve the same level of crystallinity found in the neat PP samples. The crystalline orientation was also higher in compatibilized nanocomposite samples in comparison with uncompatibilized samples.

Sonic moduli

The variation of the sonic moduli for different nanocomposite filaments is shown in Figure 4. The significant increase in the sonic moduli indicated elastic behavior becoming dominant over the viscous part in the nanocomposites. The uncompatibilized samples, however, did not show any marked increase in the sonic modulus. This argument was further supported by the much enhanced storage moduli for the compatibilized nanocomposite filaments, as discussed in the dynamic mechanical analysis study.

TABLE III
X-ray Crystallinity and f_c Values for PP/Clay Nanocomposite Filaments

Sample code	X-ray crystallinity (%)	f_c
PP	65	0.91
PPc05g00	51	0.83
PPc10g00	53	0.79
PPc025g00	53	0.81
PPc025g025	63	0.91
PPc025g05	62	0.85
PPc025g075	52	0.91
PPc05g00	51	0.83
PPc05g05	55	0.85
PPc05g10	62	0.89
PPc05g15	60	0.86
PPc10g00	53	0.79
PPc10g10	55	0.86
PPc10g20	61	0.90
PPc10g30	58	0.89

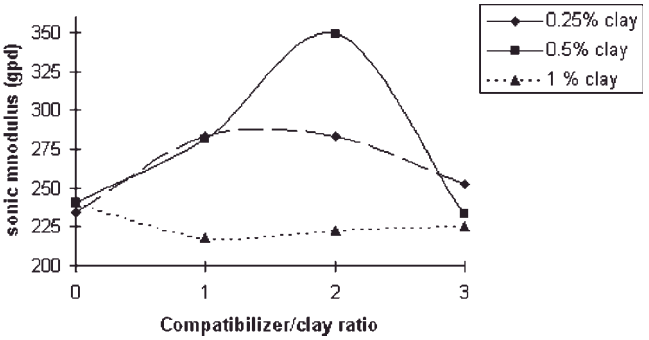

Figure 4 Sonic moduli of PP/clay nanocomposite filaments at various compatibilizer/clay loadings (neat PP filament value is ~ 234 gpd).

DSC

Table IV shows the effects of the clay and compatibilizer loadings on the T_m and crystallinity values obtained by DSC. The presence of clay affected both the melting and crystallization behavior. The clay was not dispersed homogeneously in the absence of the compatibilizer and led to much reduced crystallinity values. However, the nanolevel-dispersed clay in the presence of the compatibilizer induced heterogeneous crystallization in the filament and hence increased the crystallinity as well as the rate of crystallization. Wang et al.[19] in their study of PP/OMMT hybrid fibers also reported significant increases in the X-ray crystallinity and crystallization rate in the presence of clay. A possible reason is that the addition of OMMT promoted the nucleation and growth of the crystals and perfected the α-crystalline form. The melting point decreased slightly upon the addition of only the clay, but the effect was offset in the presence of the compatibilizer in the compatibilized PP/nanoclay filament samples. Similar findings have been reported by other researchers[22] for PP/organoclay nanocomposites, and it has been suggested that an overall reduction in the size of the lamellae is responsible for it; the clay tactoids present in the uncompatibilized system form an obstacle, thereby retarding the growth of individual lamellae.

TABLE IV
DSC Analysis

	DSC data		
Sample code	T_m (°C)	ΔH (J/g)	Crystallinity (%)
PP	167.1	133.8	64
PPc00g10	163.3	119.1	57
PPc025g025	167.3	131.7	63
PPc025g05	169.2	131.7	63
PPc05g00	166.0	112.9	54
PPc05g05	166.7	123.3	59
PPc05g10	163.8	129.6	62
PPc10g00	165.7	112.9	54
PPc10g20	161.9	127.5	61

TABLE V
TGA Analysis

Sample code	Maximum-weight-loss temperature (°C)
PP	348
PPc05g10	362
PPc10g20	387
PPc05g00	363
PPc10g00	350

Thermal stability

The TGA studies of neat PP and the nanocomposite filaments showed that the temperature of the maximum weight loss increased significantly in the nanocomposite filaments, as shown in Table V. The introduction of clay platelets increased the thermal resistance of the polymer because clay is an inherently thermally resistant material and further helps to reinforce the thin char layer that forms in PP/clay nanocomposites.[23]

Shrinkage behavior

The drawn filaments were semicrystalline and oriented but exhibited thermal shrinkage when they were heated to temperature above the glass-transition temperature (T_g) but still well below T_m because of the molecular relaxation of the polymer chains. The magnitude of the orientation depends on structural parameters such as the orientation and crystallinity of the fibers and external factors such as the temperature, tension, and time. Thus, the drawn and unset fibers possessed good tenacity and elasticity properties but had poor dimensional stability. The samples were therefore heat-set to reduce the shrinkage.

All the nanocomposite filaments showed much lower thermal shrinkage, as observed in the TMA studies (Fig. 5). The inclusion of the nanoclay in the PP matrix led to a large reduction in the thermal shrinkage in comparison with neat PP. The higher the

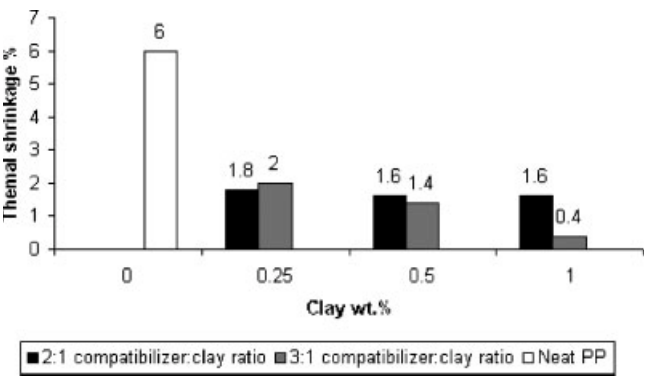

Figure 5 Thermal shrinkage of PP and PP/clay nanocomposite filaments.

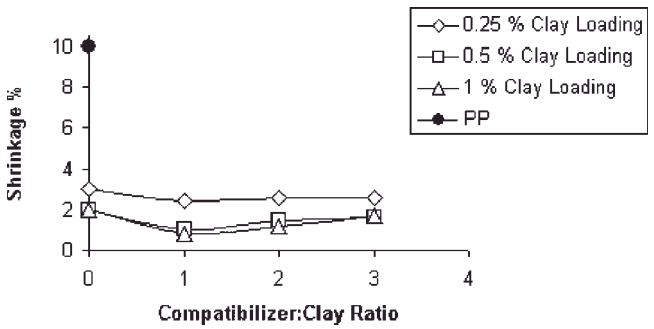

Figure 6 Boiling water shrinkage of PP and PP/clay nanocomposite filaments.

clay loading was, the greater the decrease was in the thermal shrinkage, but increasing the compatibilizer/clay ratio slightly increased the shrinkage value. There was also a marked reduction in the boiling water shrinkage of compatibilized PP/clay nanocomposite samples in comparison with neat PP (Fig. 6).

Thus, the PP/nanoclay compatibilized filaments showed improved dimensional stability under hot and hot and wet conditions. The reason could be that the dispersed clay platelets hindered the relaxation of PP molecular chains because of the reduced mobility in the interfacial regions and thus exhibited reduced shrinkage.

Mechanical properties

Tensile behavior

The tensile test results for PP and PP/clay nanocomposite filaments are shown in Table VI. The tenacity value for the fully drawn neat PP filament was 7.2 gpd, whereas for 0.5 and 1% clay loadings without the compatibilizer, it was 7.4 and 7.6 gpd, respectively. Upon the addition of the compatibilizer along with the clay (0.25–0.5 wt %) at a compatibilizer/clay ratio of 1 : 1 or 2 : 1, there was a remarkable increase (30%) in the tenacity values over neat PP. PPc025g025 showed a value of 9.46 gpd, and PPc05g10 showed a value of 9.11 gpd. The tenacity values, however, tended to stabilize or decrease at higher compatibilizer loadings.

The compatibilized PP/nanoclay filaments also showed higher tensile modulus. In the absence of the compatibilizer, there was virtually no increase in the modulus, but there was a significant increase (70%) in the tensile moduli of the compatibilized filaments. In fact, samples PPc05g10 and PPc05g15 exhibited tensile moduli of 193 and 194 gpd, respectively, versus 113 gpd for neat PP. The elongation at break was, however, marginally reduced in the nanocomposite samples in comparison with the neat PP filament.

Several studies on compatibilized PP/clay nanocomposites[1,2,16,22] in film or molded forms have reported similar increases in the mechanical properties. Xiaohui and Quiju[2] reported a 27% increase in the tensile strength and a 42% increase in the tensile modulus with a 7 wt % clay concentration for PP/clay nanocomposite samples prepared via grafting and melt compounding with a cointercalated organophilic clay. However, in this study, a much higher improvement in the tensile strength (30%) and modulus (70%) was obtained at very low loadings of 0.25–0.5 wt % clay and at a compatibilizer/clay ratio of 2 : 1. It is known that a nanometer dispersion of silicate layers in the matrix leads to improved modulus and strength. The stiffness of the silicate layers contributes to the presence of immobilized or partially immobilized polymer phases, mainly in the interphase regions,[24] which contribute to much enhanced tensile properties of the nanocomposites. The much enhanced improvements in the tensile strength and modulus in the filament that formed at very low clay loadings may have been due to the orientation of silicate layers as well as the molecular chains achieved during spinning and drawing, which contributed to the observed

TABLE VI
Tensile Properties of PP/Clay Nanocomposite Filaments

Sample code	Tenacity (gpd)	Tensile strength (MPa)	Modulus (gpd) at 1% extension	Tensile modulus (GPa) at 1% extension	Breaking elongation (%)
PP	7.2	578	113	9.1	11.1
PPc00g10	6.3	506	84	6.7	12.8
PPc00g20	7.2	578	130	10.4	10.1
PPc05g00	7.4	595	99	8.0	12.1
PPc10g00	7.6	610	112	9.0	11.4
PPc025g025	9.46	760	131	10.5	10
PPc025g05	8.09	650	141	11.3	7.4
PPc05g10	9.01	724	190	15.3	7.61
PPc05g10	9.11	732	193	15.5	7.66
PPc05g15	9.04	726	194	15.6	7.52
PPc10g20	8.4	675	136	10.9	11.3
PPc10g10	6.81	547	118	9.5	7.3
PPc10g30	6.04	485	125	10.0	8.4

reinforcement effects in the filaments at 0.25–0.5 wt % clay loading. The lowering of values above 1 wt % clay loading in our samples was due to unavoidable aggregation of the silicate layers at higher clay concentrations (> 1 wt %).

Dynamic mechanical analysis

For load-bearing applications in which stress is applied for a longer period of time, the study of viscoelastic behavior becomes important. Figures 7 and 8 show the variation of the storage modulus and tan δ, respectively, for neat PP and various PP/clay nanocomposite filaments. A marked rise in the storage moduli and decrease in the tan δ values of the nanocomposites versus the neat PP filaments over the entire temperature range can be observed (Figs. 7 and 8). In fact, some of the samples (PPc025g025 and PPc05g10) showed a 2-order rise in the storage moduli. The increase in the storage moduli indicated the growing predominance of the elastic component in the nanocomposite filaments. Thus, the presence of intercalated/exfoliated silicate clay layers increased the thermomechanical stability of the nanocomposite filaments at higher temperatures.

Jisheng et al.[16] reported an approximately threefold increase in the storage modulus of PP/clay nanocomposites at an 8% clay concentrations at temperatures higher than T_g, whereas in this study, a 2-order increase was obtained in the storage modulus values for lower concentrations of clay (0.25–0.5 wt %) at a compatibilizer/clay ratio of 2 : 1. This significant

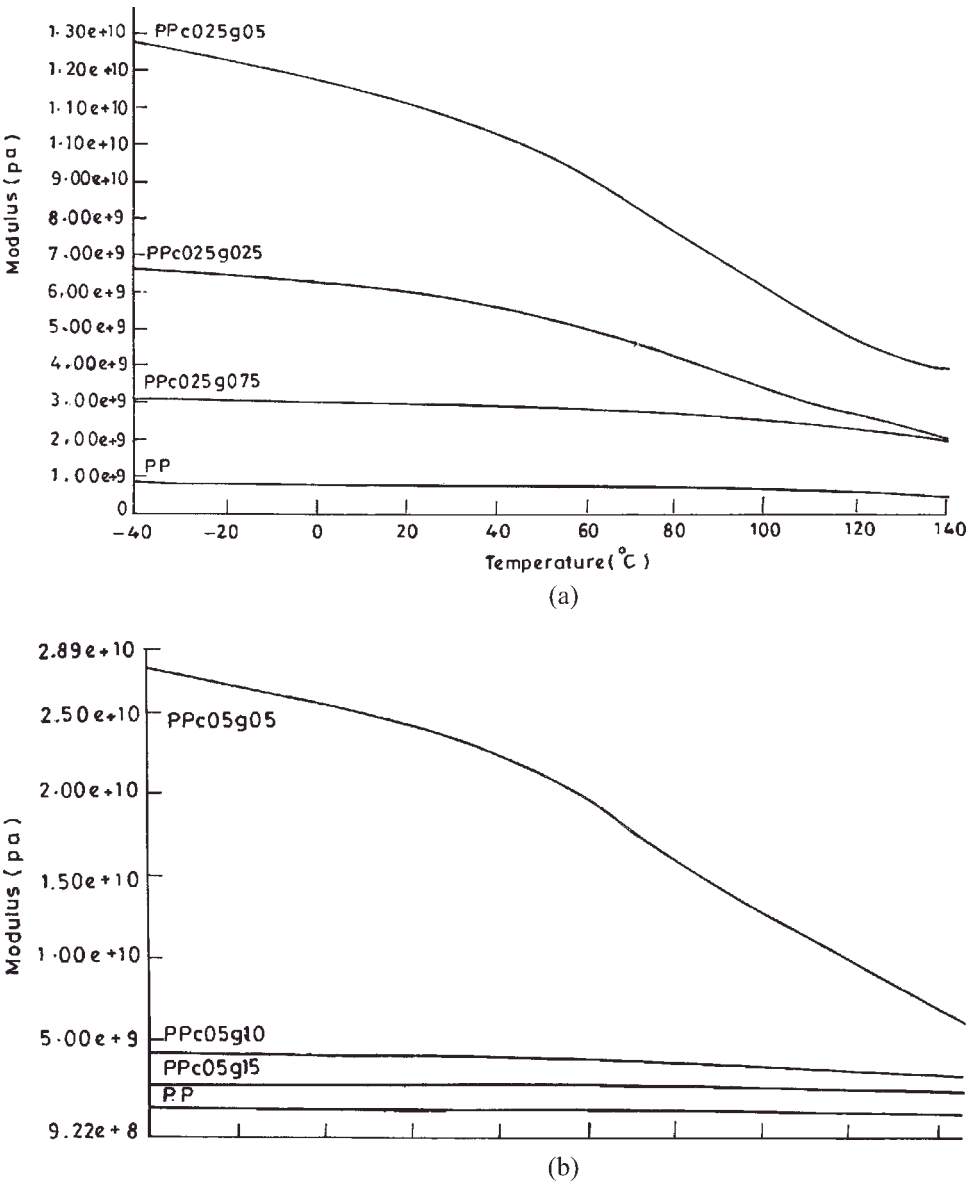

Figure 7 Storage modulus for (a) 0.25 and (b) 0.5 wt % clay loadings for neat PP and nanocomposite filaments with various compatibilizer/clay ratios.

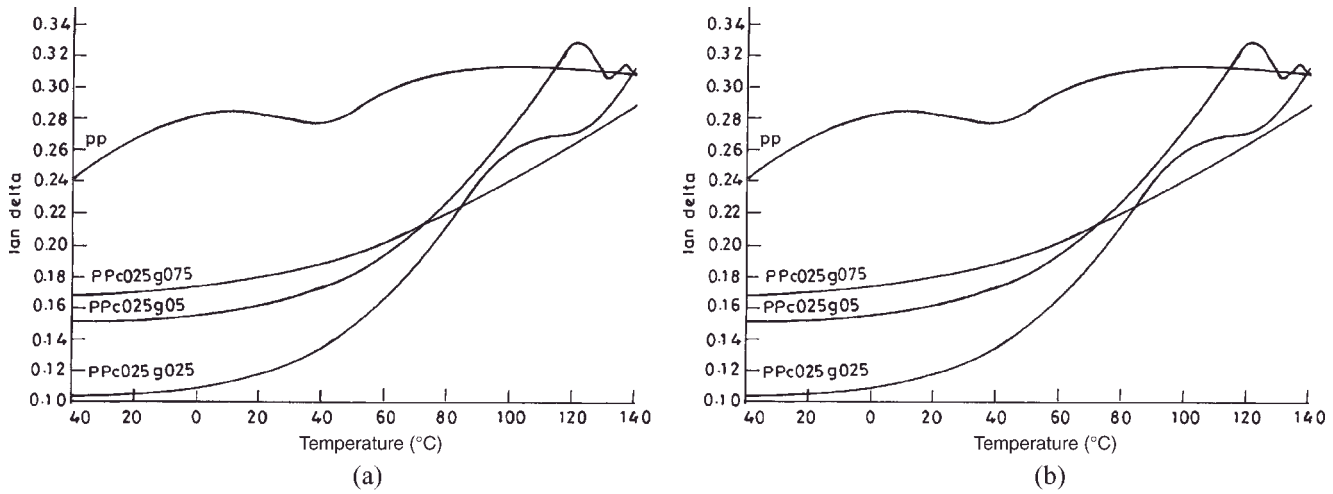

Figure 8 Tan δ for (a) 0.25 and (b) 0.5 wt % clay loadings for neat PP and nanocomposite filaments with various compatibilizer/clay ratios.

increase in the storage modulus may have been due to the immobilized or restricted mobility in the interphase regions because of clay–polymer interactions.[24] A slight shift in the β transition (T_g) to a higher temperature in the case of the PP05 and PP10 samples was observed. Other researchers have also reported small increases in T_g of PP/clay nanocomposites.[16]

Creep behavior

Because T_g of PP is below room temperature (ca. −10°C), it has a tendency to creep at and above room temperature at rather low stresses. This becomes a limitation in most applications, particularly ropes, woven sacks, polygrass, geotextiles, upholstery, and filter fabrics. There have been several attempts to enhance the creep resistance of PP via crosslinking, copolymerization, and the use of additives and fillers.[1] The results for the creep analysis of the neat PP and nanocomposite filaments are shown in Figure 9. PP showed an extension of about 4% before it stabilized, but the nanocomposite filaments exhibited almost half that value (~ 2% extension). The PP/nanoclay compatibilized filaments thus showed improved creep resistance over PP filaments for all the compositions, although the long-time prediction of the creep behavior of the nanocomposites requires the determination of the master curves and shift factor and needs further investigation.

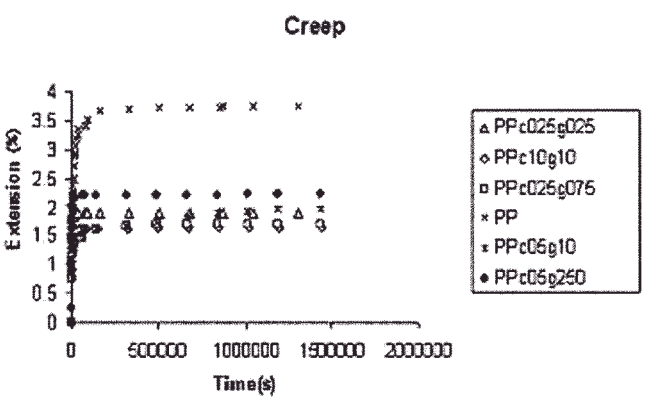

Figure 9 Creep data for PP and PP/clay nanocomposite filaments.

CONCLUSIONS

This study has demonstrated that compatibilized PP/clay nanocomposite filaments can be successfully spun and drawn into filament form up to a 1 wt % clay loading. The fibers can be drawn to a very high draw ratio (~13) with a three-stage drawing process. The incorporation of the nanoclay into the PP matrix, especially in the presence of a compatibilizer, PP-*g*-MA, leads to a tremendous improvement over a wide range of properties at very low weight fractions of the clay. A marked improvement in the tensile properties, that is, the tensile strength (30%) and tensile modulus (70%), and in the dynamic mechanical properties, that is, the storage modulus, tan δ, and creep resistance, and reduced thermal and boiling water shrinkage have been achieved at very low loadings of the clay (0.25–0.5 wt %) and at a compatibilizer/clay ratio of 2 : 1 in comparison with neat PP fibers. These superior performance properties of the PP/nanoclay compatibilized filaments provide an edge over conventional PP for use in various technical textile applications.

References

1. Gupta, V. B. Indian J Fiber Text Res 1997, 22, 236.
2. Xiaohui, L.; Quiju, W. Polymer 2001, 42, 10013.

3. Michael, A.; Philippe, D. Mater Sci Eng 2000, 28, 1.
4. Schadler, L. S. In Nanocomposite Science & Technology; Ajayan, P. M.; Schadler, L. S.; Braun, P. V., Eds.; Wiley-VCH: Weinheim, 2003.
5. Yano, K.; Usuki, A.; Okada, A.; Kurauchi, T.; Kamigaito, O. J Polym Sci Part A: Polym Chem 1993, 31, 983.
6. Ray, S. S.; Okamoto, M. Prog Polym Sci 2003, 28, 1539.
7. Mukul, B.; Ray, S. S. Adv Polym Sci 2000, 155, 169.
8. Giannelis, E. P. Adv Mater 1996, 8, 29.
9. Vaia, R. A.; Ishii, H.; Giannelis, E. P. Chem Mater 1993, 5, 1694.
10. Garcia-Lopez, D.; Picazo, O.; Merino, J. C.; Pastor, J. M. Eur Polym J 2003, 39, 945.
11. Zhiqi, S.; Simon, G. P.; Yi-Bing, C. Polymer 2002, 43, 4251.
12. Gopakumar, T. G.; Lee, J. A.; Kontopoulou, M.; Parent, J. S. Polymer 2002, 43, 5483.
13. Weibing, X.; Guodong, L.; Hongbo, Z.; Shupei, T.; Guopei, H.; Pan, W. P. Eur Polym J 2003, 39, 1467.
14. Vaia, R. A.; Klaus, D.; Karmer, E. J.; Giannelis, E. P. Macromolecules 1995, 28, 8080.
15. Kawasumi, H.; Usuki, A.; Okada, A. J Appl Polym Sci 1998, 67, 87.
16. Jisheng, M.; Zongneng, Q.; Youliang, Q. J Appl Polym Sci 2001, 82, 3611.
17. Tjong, S. C.; Meng, Y. Z.; Hay, A. S. Chem Mater 2002, 14, 44.
18. Mlynarcikova, Z.; Kaempfer, D.; Thomann, R.; Mulhaupt, R.; Borsig, E.; Marcincin, A. Polym Adv Technol 2005, 16, 362.
19. Zhang, X.; Yang, M.; Zhao, Y.; Zhao, S.; Dong, X.; Liu, X.; Wang, D.; Xu, D. J Appl Polym Sci 2004, 92, 552.
20. Joshi, M.; Butola, B. S.; Shaw, M. Fibers Polym 2004, 5, 1.
21. Morgan, A. B.; Gilman, J. W. J Appl Polym Sci 2003, 87, 1329.
22. Suboda, P.; Zeng, C.; Wang, H.; Lee, L. J.; Tomasko, D. L. J Appl Polym Sci 2002, 85, 1562.
23. Qin, H.; Zhang, Z.; Zhao, C.; Hu, G.; Yang, M. Polymer 2005, 46, 8386.
24. Traganopoulos, G.; Eisenberg, A. Macromolecules 1995, 28, 6067.